Strong Effects of Molecular Structure on Electron Transport in Carbon/Molecule/Copper Electronic Junctions

Franklin Anariba, Jeremy K. Steach, and Richard L. McCreery*

Department of Chemistry, The Ohio State University, 100 West 18th Avenue, Columbus, Ohio 43210

Received: March 3, 2005; In Final Form: April 8, 2005

Carbon/molecule/copper molecular electronic junctions were fabricated by metal deposition of copper onto films of various thicknesses of fluorene (FL), biphenyl (BP), and nitrobiphenyl (NBP) covalently bonded to flat, graphitic carbon. A "crossed-wire" junction configuration provided high device yield and good junction reproducibility. Current/voltage characteristics were investigated for 69 junctions with various molecular structures and thicknesses and at several temperatures. The current/voltage curves for all cases studied were nearly symmetric, scan rate independent, repeatable at least thousands of cycles and exhibited negligible hysteresis. Junction conductance was strongly dependent on the dihedral angle between phenyl rings and on the nature of the molecule/copper "contact". Junctions made with NBP showed a decrease in conductivity of a factor of 1300 when the molecular layer thickness increased from 1.6 to 4.5 nm. The slope of ln(*i*) vs layer thickness for both BP and NBP was weakly dependent on applied voltage and ranged from 0.16 to 0.24 $Å^{-1}$. These attenuation factors are similar to those observed for similar molecular layers on modified electrodes used to study electrochemical kinetics. All junctions studied showed weak temperature dependence in the range of approximately 325 to 214 K, implying activation barriers in the range of 0.06 to 0.15 eV. The carbon/molecule/copper junction structure provides a robust, reproducible platform for investigations of the dependence of electron transport in molecular junctions on both molecular structure and temperature. Furthermore, the results indicate that junction conductance is a strong function of molecular structure, rather than some artifact resulting from junction fabrication.

Introduction

The promise of incorporating molecules into microelectronic devices has stimulated a variety of approaches to making metal/molecule/metal electronic junctions. To date the vast majority of molecular junctions are based on self-assembled monolayers (SAMs)[1,2] and Langmuir−Blodgett (LB)[3−6] structures in which the bonding between a metallic contact and a molecular monolayer is either a Au−S or an electrostatic bond. For example, SAM junctions have been investigated by making contact to a monolayer on a metal with mercury drops,[7−12] by depositing metals through low-temperature evaporation,[1,13,14] by electroless[15] or electrochemical deposition,[16,17] and by employing scanning probe microscopy tips as the metal top contact.[18−25] Top metal contacts for LB junctions include Al or Al oxide,[26−29] titanium,[3,5,30−33] and Au metal.[27] Carbon nanotube[34,35] and metallic nanowires[16,17,36−39] have also provided significant insight into the control of electron transport in molecular structures, and electronic devices such as nonvolatile random access memory and one-dimensional array nanostructures have been demonstrated.

A major goal of research in molecular electronics is the correlation of molecular structure with electron transport behavior, since such a correlation provides strong evidence that observed electronic effects are *molecular* and not some artifact of the device or measurement. In donor−bridge−acceptor molecules,[40−43] electron transfers through monolayers in electrochemical cells[44−49] and in scanning probe microscopy experiments,[19,24,25,50−55] electron transport has been shown to depend strongly on the length, conjugation, conformation, and substituents of the molecule(s) through which electron transfer occurs. Such correlations have proven difficult in metal/molecule/metal junctions, however, partly due to poor junction yield and a variety of electronic effects observed for junctions of nominally identical design. Junction fabrication is difficult for a variety of reasons, including penetration of the metal top contact through the molecular layer, degradation of the molecule during metal deposition, and the presence of metal oxides within the junction.[20,56−61] The primary motivation for the current work was to establish a reproducible, robust junction design which would allow investigation of the effects of molecular structure on electronic behavior. If junction electronic properties consistently and strongly depend on monolayer molecular structure, it is certain that the molecule is playing a role in electron transport.

We have reported several examples of carbon-based molecular junctions, in which a carbon−carbon covalent bond replaces the Au−thiol bond in SAMs or the electrostatic bond in LB structures.[62−70] The carbon-based approach offers several distinct features that permit fabrication of reproducible molecular junctions via vapor deposition of a metal or metal oxide top contact on a molecular layer bonded to a graphitic carbon substrate. First, the C−C bond between the substrate and the organic layer forms irreversibly and is symmetric and strong (∼100 kcal/mol) compared to Au−S (40 kcal/mol) and LB films (<10 kcal/mol). The pyrolyzed photoresist film (PPF) substrate is structurally and electronically similar to glassy carbon, with a very flat surface (<0.5 nm rms roughness) and a resistivity

* Corresponding author. Telephone: 614-292-2021. E-mail: mccreery.2@osu.edu.

10.1021/jp051093f CCC: $30.25
Published on Web 05/11/2005

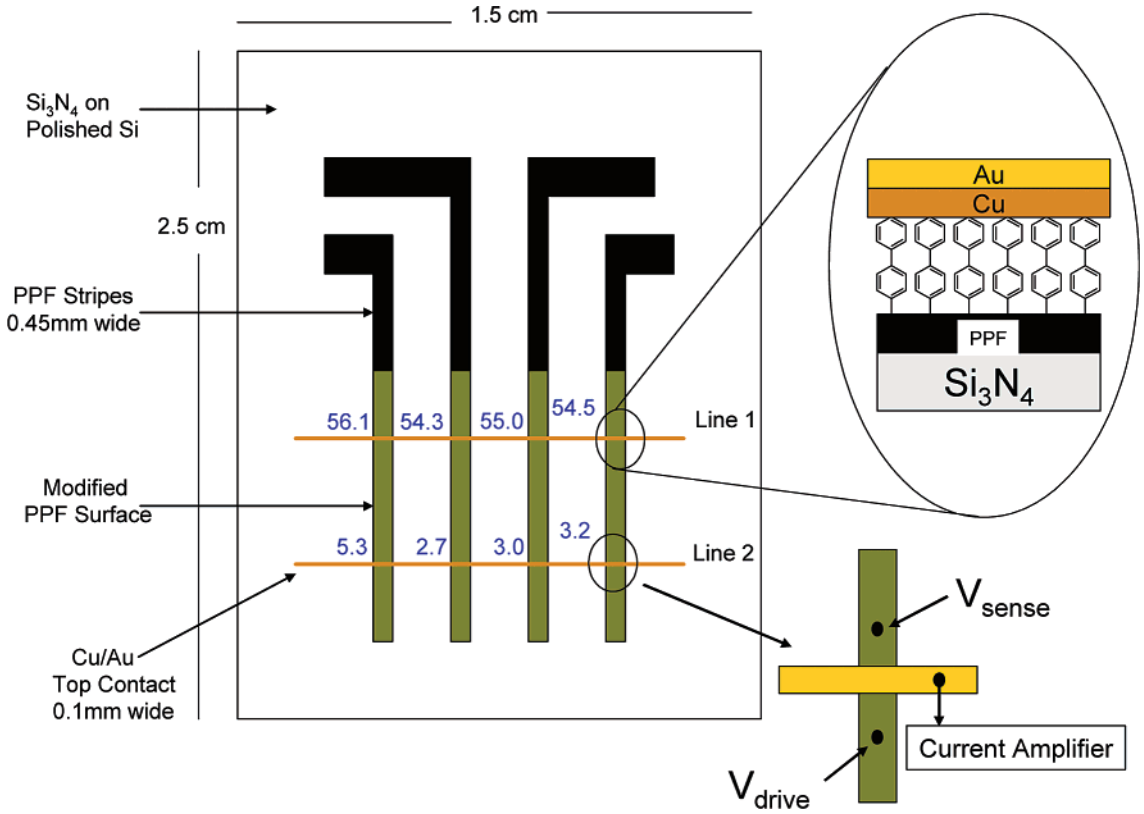

Figure 1. Schematic of PPF/molecule/Cu/Au molecular junction sample. Numbers adjacent to each junction are the observed low-voltage (±50 mV) resistances in kiloohms for BP multilayer (1.9 nm, line 1; BP monolayer (1.5 nm), line 2. Inset in lower right shows contacts to the junction in a three-wire configuration, with the *iR* corrected junction voltage equal to V_{sense} relative to the metal strip at virtual ground.

of 0.005 Ω·cm.[71−74] Second, diazonium reduction on carbon surfaces has been shown by X-ray photon spectroscopy (XPS), Raman, Fourier transform infrared (FTIR), atomic force microscopy (AFM), and scanning tunneling microscopy (STM) to result in high coverage of covalently bonded organic molecules, with very low pinhole density.[75−94] Since possible pinholes are sites for phenyl radical formation, they are actively "patched" by the newly formed radical. Third, carbon-based molecular junctions are amenable to in-situ Raman spectroscopy through a partially transparent metal top contact, permitting verification of structure and observation of bias-induced structural changes.[67,69] Finally, the monolayer is robust enough that metal deposition can be accomplished without apparent monolayer damage or the formation of metal filaments.[65,68] The junction geometry used here is similar to "cross-bar" or "crossed-wire" junctions,[26,33,34,95,96] with a molecular layer bridging the gap between two conventional conductors. The junction structure in the current work has a graphitic carbon substrate and a Cu/Au top contact in a crossed-wire configuration in all cases. Within the confines of a given junction design, molecules were chosen which would reveal the effect of small changes in structure (biphenyl vs fluorene), top contact bonding (biphenyl vs nitrobiphenyl), and molecular layer thickness (nitrobiphenyl, 1.6−4.5 nm) on the electronic behavior of the molecular junctions. In other words, for monolayers of comparable thickness, we were interested in determining how conductivity is affected by changes in molecular structure. Furthermore, the dependence of conductivity on film thickness was also investigated for multilayers of BP and NBP.

Experimental Section

Molecular junctions were fabricated with a procedure adapted from that reported previously,[65,66] but with "crossed-junction" rather than "spot" configuration. Polished silicon wafers with ~1000 Å thick silicon nitride coatings were cut into 15 × 30 mm pieces, which acted as insulating, flat substrates for the pyrolyzed photoresist films (PPF) that formed the bottom "contact" of the molecular junction. Cut pieces were sonicated in Nanopure water (18 MΩ·cm) for 5 min, followed by a 30 s rinse with Nanopure water and then stored in Nanopure water in a clean glass vial with a protective plastic cap for no more than 30 min. The samples were then dried in a stream of argon gas, placed in a glass Petri dish, and dried in an oven at 90 °C for 5 min. After cooling, PPF films were prepared as described previously,[73,97] except for an added lithography step before pyrolysis. Several applications of positive photoresist (AZ-P4330-RS, A−Z Electronic Materials, Sommerville, NJ) were applied by spin coating. Individual samples were then placed under a lithographic contact mask (Photo Sciences, Inc., Torrance, CA) with a pattern of four stripes 0.5 mm in width (Figure 1). A 500 W Hg arc lamp (model 68810, Oriel Corp., Stratford, CT) was used to expose the uncured photoresist to soft UV radiation for 120 s. Immediately after UV exposure, the samples were transferred to a 1:4 (v/v) solution of photoresist developer (AZ 400K, A−Z Electronic Materials) in Nanopure water for 20−30 s, then rinsed with Nanopure water, Ar-dried, and soft-baked at 90 °C for 20 min. Pyrolysis was carried out as described previously,[73,97] to 1000 °C in flowing 5% H_2 in N_2. PPF samples were prepared in batches of 2−4, with no observable effect on reproducibility. A profilometer (Detak^3 ST, Sloan) was used to determine final PPF dimensions, yielding a thickness of 1 μm and width of 0.45 mm. The resistivity of PPF film was similar to that of glassy carbon, approximately 5 × 10^{-3} Ω·cm.[73,97] Prior to surface modification, the pyrolyzed samples were sonicated in acetonitrile (Sigma-Aldrich, 99.5+%) for 5 min and dried with an Ar stream.

TABLE 1: Observed Thickness of Molecular Films Formed by Diazonium Reduction

molecule	sample[a]	line	AFM thickness,[b] nm	yield[c]
BP-2	1	1[e]	1.54 ± 0.25	4/4
BP-2	1	2	1.86 ± 0.33	4/4
BP-2	2	1	1.82 ± 0.32	4/4
BP-2	2	2	2.87 ± 0.29	4/4
BP-2	3	1	1.60 ± 0.29	4/4
BP-2	3	2	1.85 ± 0.17	4/4
FL-1	4	1	2.17 ± 0.28	3/4
FL-1	4	2	1.71 ± 0.27	4/4
FL-1	5	1	1.80 ± 0.21	4/4
FL-1	5	2	1.74 ± 0.17	4/4
NBP-1	6	1	2.07 ± 0.26	2/4
NBP-1	6	2	1.66 ± 0.09	3/4
NBP-1	7	1	1.78 ± 0.19	4/4
NBP-1	7	2	1.66 ± 0.14	4/4
NBP-4	8	1	2.80 ± 0.31	4/4
NBP-10	9	1	3.77 ± 0.17	4/4
NBP-20	10	1	4.51 ± 0.44	4/4
NBP-20	11	1	4.33 ± 0.18	4/4

[a] "Sample" refers to independently prepared substrate/PPF/molecule samples. [b] Mean ± standard deviation, based on 10 AFM profiles through an intentional scratch in the molecular layer (see ref 94). Scratch was positioned immediately adjacent to a junction, on the PPF. [c] Junctions were rejected if the second *i*/*V* scan differed significantly from the first. [d] Number of derivatization scans, all at 0.2 V/s, starting at +0.4 V vs Ag/Ag^+, and then to the negative potential indicated and back to +0.4 V. Negative limits for scans were as follows: BP, −1.0 V; FL, −0.8 V; NBP-1 and NBP-4, −0.6 V; NBP-10 and −20, −0.9 V. [e] "Line" refers to the upper or lower metal lines, as shown in Figure 1.

Electrochemical derivatization was performed with a BAS 100 W potentiostat (Bioanalytical Systems, West Lafayette, IN), as described previously.[65,94] An Ag^+/Ag (0.01 M; Bioanalytical Systems) reference electrode calibrated with ferrocene to be +0.22 V vs aqueous SCE was used for derivatization. Modification of PPF surfaces was carried out by the reduction of a 1 mM solution of the corresponding diazonium salt in 0.1 M *n*-tetrabutylammonium tetrafluoroborate ($(TBA)BF_4$, Sigma-Aldrich 99.5%+) in acetonitrile. Each diazonium reagent was synthesized within 1 month of use and stored in a freezer as a solid fluoroborate salt. Diazonium salt solutions were freshly prepared and degassed thoroughly with Ar for 20 min. Monolayers of FL, BP, and NBP, as well as multilayers of NBP, were deposited as indicated in Table 1. Film thicknesses were verified with AFM "scratching" as described elsewhere,[94] with the results listed in Table 1. When junctions are identified in the text and figures, the AFM-determined molecular layer thickness is indicated in parentheses in nanometers, e.g. BP(1.5). The AFM technique was shown to yield thickness consistently higher than that expected from the geometric size of a perpendicularly oriented molecule by 0.3−0.4 nm, presumably due to a layer of adsorbed water.[94] AFM thicknesses between 1.5 and 1.7 nm in Table 1 indicate monolayers of BP, NBP, or FL (which have geometric lengths of 1.1, 1.1, and 1.2 nm) Several authors have pointed out that diazonium reduction can result in multilayer formation, due to attack of additional electrogenerated radicals on the first modification layer to yield molecular layers with thicknesses of 6 nm or more.[89,91,94,98,99] FTIR[99] and SIMS[100] results indicate formation of phenyl−phenyl bonds during coupling of additional layers beyond a monolayer, and the resulting multilayer is unlikely to be as ordered as the initial monolayer. Of the molecules in the current study, NBP forms multilayers quite readily, with the thickness depending on deposition time and potential. Table 1 includes the AFM thicknesses for several multilayers made from NBP and BP.

Following surface modification all samples were immediately transferred to a clean acetonitrile solution (Sigma-Aldrich, 99.5+%) for 60 s to remove residual diazonium salt, then rinsed in acetonitrile for 20 s, and dried with an Ar stream. Finally, samples were rinsed with isopropyl alcohol for another 20 s (Sigma-Aldrich), dried with Ar gas stream, rinsed again with acetonitrile, and finally dried with the Ar stream.

Following surface derivatization and cleaning, the modified samples were loaded into a vacuum chamber for metal deposition through a shadow mask consisting of two 100 μm wide parallel lines (see Figure 1). The mask and samples were positioned on a rotating holder ∼50 cm from the crucible of an electron-beam source (Telemark, Freemont, CA). After cryopumping to $<2.7 \times 10^{-7}$ Torr, Cu was deposited at just above the threshold current to yield a rate of 0.03−0.08 nm/s until a Cu thickness of 10 nm. An additional 20 nm of Cu was deposited at a rate of 0.35−0.55 nm/s; then Au was deposited through the same mask without breaking vacuum at 1.0 nm/s for a thickness of 10 nm. The gold layer both protected the Cu and provided good electrical contact. The dimensions of the junctions were confirmed with an optical microscope with a video measuring accessory (Olympus BX60) to be 100×450 μm, for a junction area of 4.5×10^{-4} cm^2. The sample temperature was not controlled during deposition, but the chamber temperature increased from 15 to 25 °C during metal deposition.

Each sample was comprised of either 4 or 8 crossed junctions, as shown in Figure 1. Each junction was contacted individually using three Au-plated Pt wires (MM Micromanipulator, Carson City, NV) positioned with three 3-axis micropositioners. Contact with the PPF was made with 100 μm diameter metal tips 1−4 millimeters away from the junction and with a 50 μm diameter tip wire on the more delicate Au top contact strip, about <1 mm from the junction. To compensate for ohmic losses in the PPF, the voltage was applied at V_{drive} (shown in Figure 1), but the junction voltage was monitored at point V_{sense}. Under the assumption that the Cu/Au strip remains at virtual ground, V_{sense} represents the *iR* corrected junction voltage. The resistance of the Cu/Au strip between the junction and the probe was measured to be <20 Ω, including contact resistance, resulting in a maximum uncompensated ohmic loss of 20 mV at 1 mA. This "three-wire" configuration is analogous to the three electrodes typically used by potentiostats in electrochemical experiments. The Au wire electrode was connected to a current amplifier (Keithley, model 428), and both V_{corr} and the current amplifier output were monitored simultaneously by two channels of a National Instruments model 6120 data acquisition board controlled by Labview (National Instruments).

Figure 1 shows low-voltage resistances determined from the slope of the *i*/*V* curve ($V = \pm 50$ mV) for a typical sample, in this case PPF/BP/Cu/Au. The resistances were consistent across a horizontal "line" of junctions, but there was significant variation down a given PPF line. The molecular layer thickness for a particular set of modified PPF strips in a given sample decreases down the modified PPF lines as determined by the AFM scratching technique, presumably due to ohmic losses from the PPF resistance during diazonium electroreduction. The thicknesses of the BP layer adjacent to each line of junctions are shown in Table 1. Figure 2 shows overlays of four *i*/*V* curves obtained for the junctions within each "line". Although the four monolayer junctions (1.54 nm) show a higher relative standard deviation (rsd) for the low voltage resistance (32%), the *i*/*V* curves at higher bias are very reproducible. Given the variation in layer thickness along each PPF strip, AFM was used to

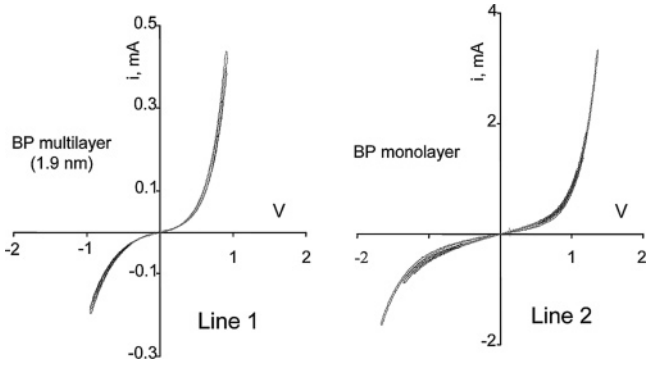

Figure 2. Overlays of *i*/*V* curves for each of the four junctions along line 1 and line 2 of the biphenyl sample shown in Figure 1. Junction area was 4.5×10^{-4} cm^2 in all cases, and the scan rate was 1000 V/s.

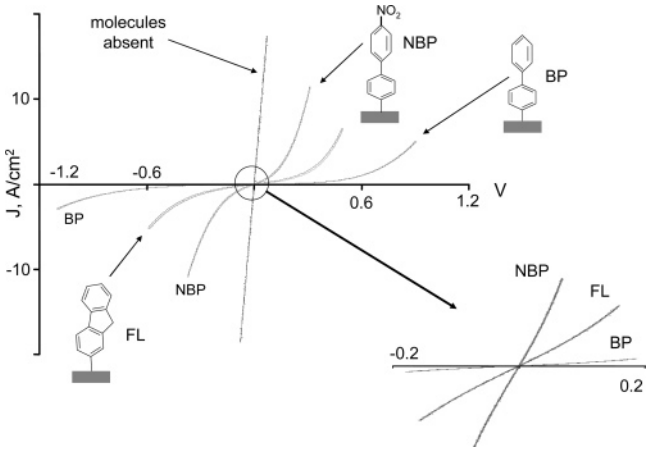

Figure 3. *J*−*V* curves for nitrobiphenyl, biphenyl, and fluorene taken at room temperature with a scan rate of 1000 V/s. Monolayer thickness as verified by AFM was 1.6, 1.7, and 1.7 nm, respectively. Inset shows expanded scale near the origin. "Molecule absent" curve in the main figure is a control junction prepared identically but without the diazonium reduction step. Each curve is an average of four junctions along a given "line".

determine the molecular layer thickness adjacent to all of the "lines" examined, as listed in Table 1.[94]

Electronic testing was carried out with a Labview-based system using a National Instruments 6120 data acquisition board. As noted earlier, a 3-wire configuration was used, with two A/D channels monitoring the current signal from a Keithley model 428 current amplifier and the *iR*-corrected applied voltage (V_{sense}, Figure 1). Except where noted, all measurements were carried out at room temperature within 1 day after fabrication. Samples rested on a Cu stage containing a thermocouple and in thermal contact with a liquid nitrogen reservoir. For temperatures above and below room temperature, the Cu stage was heated by a Digi-Sense model 68900-01 temperature controller (Eutech Instruments Pte Ltd.). A second thermocouple positioned near the sample was used to confirm the sample temperature.

Junction capacitance was measured with a Stanford Research SR720 LCR meter, using a four-wire geometry and frequencies of 0.1, 1, 10, and 100 kHz, with a drive voltage of 0.1 V.

Results

Current density vs voltage curves for monolayer junctions of nitrobiphenyl, fluorene, and biphenyl are shown in Figure 3. The inset shows a linear region at low voltage (±0.1 V) and nonlinearity at higher bias. Each of the *J*−*V* curves presented in Figure 3 is the average of four independent junctions. To

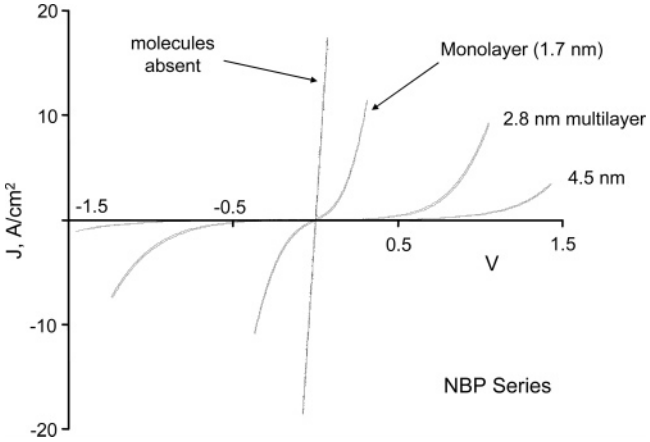

Figure 4. *J*−*V* traces for a nitrobiphenyl series of different thicknesses obtained at room temperature and a scan rate of 1000 V/s. Each curve is an average of four junctions along a given "metal line", and the NBP layer thickness determined with AFM is indicated.

avoid junction breakdown due to local heating, the scan rate was generally 1000 V/s and the current limited to <8 mA. Several PPF/molecule/Cu/Au junctions for each molecule were examined for the effect of voltage scan rate, and exhibited *i*/*V* curves which were independent of scan rate between 0.1 and 1000 V/s. A biphenyl junction cycled for 7.2 million cycles at 320 V/s exhibited no change in *i*/*V* response (data not shown). The high conductivity of the NBP monolayer junction resulted in a very high current density of 11.3 A/cm^2 at +0.31 V. The long lifetime of the samples when examined at scan rates above 100 V/s implies that the heat generated in the junction by the high current density is efficiently conducted into the relatively thick PPF and/or metal contacts. As is clear from Figure 3, the conductances of the FL and BP monolayers were lower than that of NBP, with low-voltage resistances ($V = \pm 50$ mV) as follows: NBP (1.7), 286 Ω; FL (1.7), 886 Ω; BP (1.6), 9890 Ω. Thus, for both the low-voltage region and the higher-voltage nonlinear regions of the *i*/*V* curves, the three monolayer junctions exhibited a large range of conductivity, with variations of factors of 20−35 for a variation in thickness of only 9%. In all three cases, rectification was quite small, with $J(+0.5)/J(-0.5)$ ranging between 1.0 and 2.1 for all junctions studied. The magnitude of the observed current densities and observed low-voltage junction resistances clearly indicate a strong dependence on the monolayer molecular structure.

Current density−voltage curves of a NBP series of different thickness are shown in Figure 4. The measured NBP film thicknesses were 1.66, 2.81, and 4.51 nm, as indicated. Figure 4 shows clearly that the *J*−*V* curves and junction conductivity are strongly dependent on film thickness. For example, at +0.31 V, the current density ranged from 11.3 A/cm^2 for NBP monolayer(1.7) to 0.067 A/cm^2 for NBP multilayer(2.8), and 0.0083 A/cm^2 for NBP multilayer(4.5). Therefore, a change in thickness by a factor of 2.8 caused a decrease in current density by a factor of >1300.

Table 2 lists all of the junctions and samples studied, to demonstrate the yield of working junctions. A junction was rejected only if subsequent scans after the first showed a large increase in current density. This increase appeared to result from dielectric breakdown of the molecular layer and occurred in three of the 72 junctions studied. A complete listing of low-voltage resistances and current densities is shown in Table 2, which classifies junctions according to molecular structure and film thickness. The low voltage resistance values across a given line

TABLE 2: Resistances and Current Densities for PPF/Molecule/Cu Junctions[a]

junction type	AFM[b] thickness, nm	resistance ($V = \pm 0.05$ V), KΩ	mean J, A/cm^2	
			+0.5 V [a]	−0.5 V
BP	1.54	3.6 ± 1.2	0.38 ± 0.07	0.36 ± 0.08
BP	1.60	9.90 ± 2.6	0.53 ± 0.15	0.30 ± 0.09
BP	1.82	42.1 ± 0.5	0.11 ± 0.01	0.067 ± 0.004
BP	1.85	8.74 ± 0.16	0.57 ± 0.02	0.330 ± 0.005
BP	1.86	54.9 ± 0.8	0.120 ± 0.006	0.092 ± 0.003
BP	2.87	115 ± 21	0.059 ± 0.009	0.034 ± 0.007
FL	1.71	0.886 ± 0.075	6.70 ± 0.77	3.26 ± 0.32
FL	1.74	0.514 ± 0.045	9.3 ± 1.9	4.98 ± 0.85
FL	1.80	0.682 ± 0.101	9.8 ± 1.97	4.4 ± 1.0
FL[c]	2.17	1.30 ± 0.16	4.59 ± 0.53	2.20 ± 0.22
NBP	1.66	0.286 ± 0.060	10.8 ± 1.3	6.78 ± 0.90
NBP	1.66	0.799 ± 0.058	7.2 ± 3.9	4.4 ± 2.5
NBP	1.78	0.258 ± 0.035	12.0 ± 4.7	9.3 ± 2.6
NBP[d]	2.07	1.254 ± 0.078	7.1 ± 2.9	4.1 ± 1.8
NBP	2.80	25.5 ± 0.35	0.363 ± 0.008	0.243 ± 0.008
NBP	3.77	43.4 ± 1.5	0.118 ± 0.004	0.083 ± 0.002
NBP	4.33	346. ± 5.2	0.048 ± 0.001	0.025 ± 0.001
NBP	4.51	362. ± 24	0.041 ± 0.002	0.020 ± 0.001
molecule absent	N/A	0.0090 ± 0.0001		

[a] Resistance and current density are based on four different junctions per sample unless stated otherwise. [b] AFM statistics are shown in Table 1. [c] Statistics obtained from three junctions. [d] Statistics obtained from two junctions.

of junctions exhibited relative standard deviations of 5−15% in most cases, with three of eighteen lines having rsd's above 20%.

Figure 5A is a plot of differential conductance (dI/dV) vs applied voltage for NBP, FL, and BP monolayers along with a similar plot for the series of NBP multilayers (Figure 5B). The high conductivity at high biases indicates rapid electron transport through the molecular layer, especially for NBP and FL. In no case was a plateau in the conductance vs V plots observed, and the voltage range considered was limited by the current limit of the current amplifier. To visualize a wider range of currents near $V = 0$, Figure 6A shows an overlay of ln(current) vs applied bias for NBP, FL, and BP monolayers. Each curve is an average of i/V responses for four junctions of the same molecule and thickness. Figure 6B shows a similar plot for NBP multilayer junctions having a range of thicknesses.

The well-known exponential dependence of electron tunneling on molecular layer thickness was tested by plotting ln(i) vs thickness for low voltage (0.1 V), shown in Figure 7A. The observed slopes were −0.21 Å^{-1} for BP and −0.22 Å^{-1} for NBP. Each point shown in Figure 7 is the average of four junctions, with the error bars indicating the standard deviations. Similar plots were constructed for various bias voltages, and the slopes are shown in Figure 7B. For BP junctions of various thicknesses, the slope decreases slightly with applied voltage, while that for NBP is comparatively constant with bias. The results for FL were not analyzed in this fashion because too few film thicknesses were available.

The temperature dependence of the i/V curves was examined over a range of approximately 214 to 325 K, with the results shown in Figure 8. Although such temperature effects were quite reproducible, the curves in Figure 8 were determined from one junction of each type. In all cases, the current decreased with decreasing temperature, at a rate which was similar for BP, FL, and NBP monolayers and NBP multilayers. The changes with temperature were completely reversible upon returning the junction to room temperature, at least for the temperature and voltage ranges studied. The capacitance of all junctions, as measured with an LCR meter, decreased with increasing

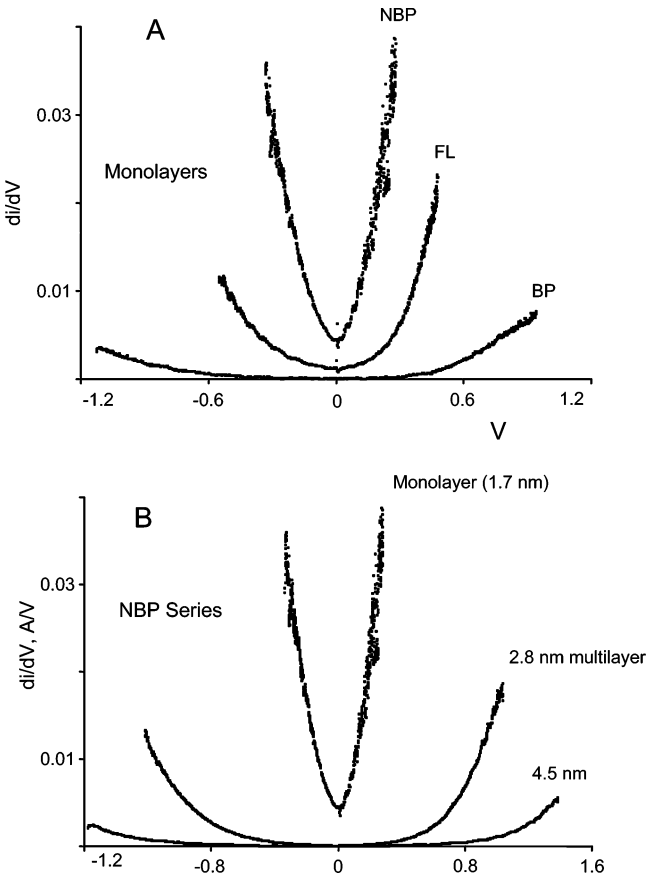

Figure 5. (A) Differential conductance (di/dV) for nitrobiphenyl, fluorine, and biphenyl monolayers at room temperature and a scan rate of 1000 V/s. (B) Similar plot for a nitrobiphenyl series of various thicknesses. Differential conductance was determined as the slope of the i/V curve for ∼10 mV segments of the i/V curves.

frequency. For example, a typical NBP multilayer 4.5 nm thick junction had an observed capacitance of 7.7, 6.7, 4.4, and 2.1 μF/cm^2 for 0.1, 1, 10, and 100 kHz, respectively. At 100 kHz, all junctions studied had capacitances in the range of 2.1−3.3 μF/cm^2, and the capacitance decreased as molecular layer thickness increased for the NBP multilayer series. The frequency dependence of observed capacitance may be due to the relatively low junction resistance, which makes accurate measurement of the capacitive current difficult.

Discussion

The high yield and reproducibility of the crossed-junction design shown in Figures 1 and 2 is at least partly the result of the strong C−C bond between the substrate and molecular layer. Irreversible formation of a ∼100 kcal/mol bond by diazonium reduction apparently prevents penetration of vapor-deposited Cu, as has been reported for the Au/thiol and Langmuir−Blodgett monolayers. Since the monolayer molecules are immobile and densely packed, they are unable to move laterally to permit metal incursion.[67,69] The crossed-junction design also avoids direct physical contact between the probes and the junction, and a three-wire configuration corrects for possible variation in wire/PPF contact resistance. The higher current densities observed with the current junctions compared to those reported previously are largely a consequence of the correction of ohmic losses in the PPF.

The dependence of junction conductance on structure shown in Figures 3 and 4 provides strong evidence that metallic "short circuits" or pinholes in the molecular layer do not contribute

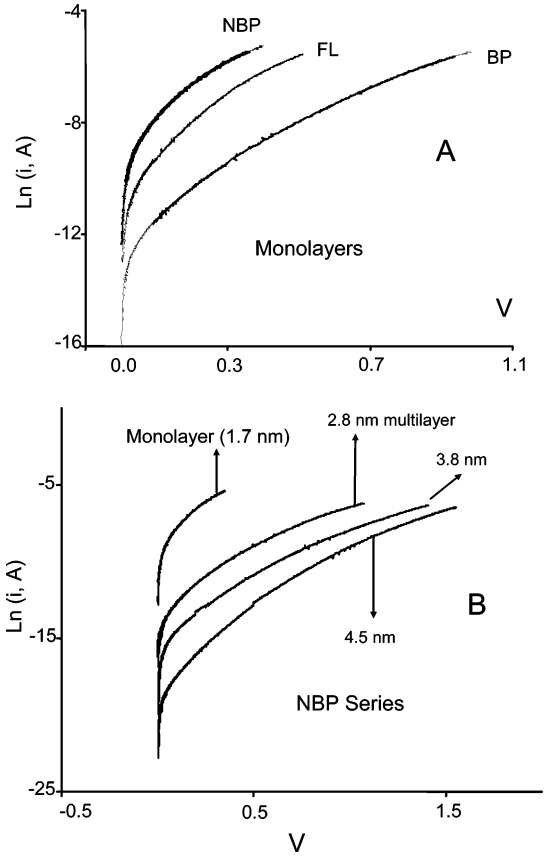

Figure 6. (A) ln(*i*) vs *V* for nitrobiphenyl, fluorene, and biphenyl monolayers obtained at room temperature and a scan rate of 1000 V/s. (B) ln(*i*) vs *V* for a series of nitrobiphenyl thicknesses acquired under the same conditions. Layer thickness is indicated in nanometers.

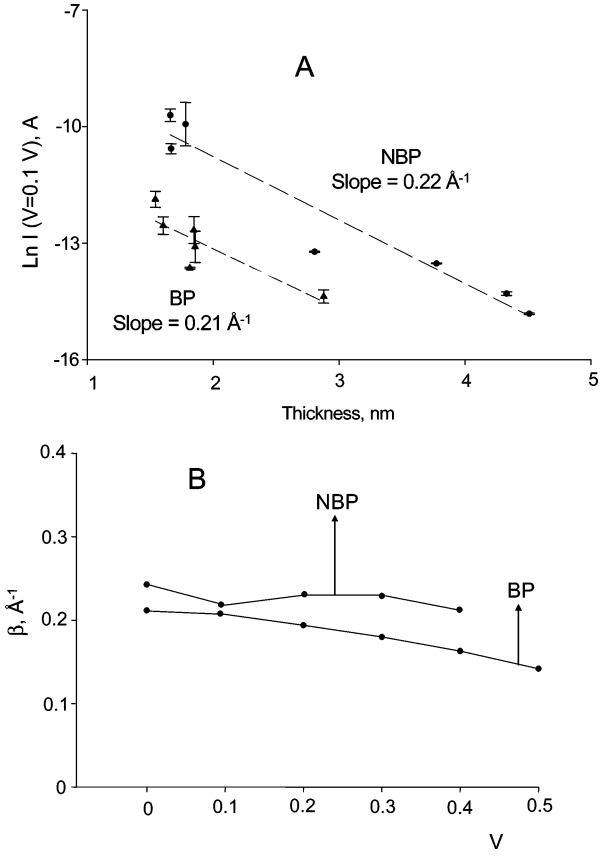

Figure 7. (A) Plots of the natural log of the current at $V = +0.1$ V vs molecular layer thickness for BP and NBP. (B) Absolute value of slope (β) of ln(*i*) vs thickness plots at several bias voltages for both biphenyl and nitrobiphenyl. Each point is an average of four junctions.

significantly to junction electronic characteristics. Biphenyl, fluorene, and nitrobiphenyl monolayer junctions with similar thicknesses (1.6, 1.7, and 1.7 nm, respectively) have very different low-voltage resistances, varying from 9893 Ω for BP to 286 Ω for NBP. Comparing FL to BP, the only structural change is a bridging CH_2 group which forces the phenyl rings of FL to be coplanar. FL and BP junctions have the same bonding to PPF, the same contact with Cu, the same thickness, and nearly identical compositions. However, the FL junction is 11 times more conductive than the BP junction at low voltage, and 12.5 times more conductive at +0.5 V. If metallic "shorts" were present, they might be expected to be more prevalent for the BP case, since its ~36° dihedral angle should lead to less dense packing in the monolayers. However, any packing differences between BP, NBP, and FL were not apparent by AFM and in any case would be much smaller than the observed differences in conductivity. The fact that conductivity is sensitive to the planarity of the phenyl rings is very difficult to explain with metallic shorts or coverage differences. Furthermore, the much higher conductivity of NBP compared to BP junctions (a factor of 35 higher at +0.5 V) is consistent with reports that a covalent bond at both ends of the molecule enhances conductivity[23,55,101] but is not consistent with metal incursion into the monolayer. A reactive end group has been shown to prevent incursion by reacting with the vapor-deposited metal,[58−61] and the nitro group of NBP is likely to form a covalent bond with Cu, as has been observed for Ti deposited on nitroazobenzene.[67,69]

Figure 4 shows the strong thickness dependence for NBP with a factor of >1300 decrease in conductivity for an increase in thickness from 1.7 (monolayer) to 4.5 nm (multilayer). Such behavior is not expected for metallic filaments, unless the filament density decreases rapidly with molecular layer thickness. Furthermore, metallic filaments should behave as ohmic conductors, with linear *i*/*V* curves and an inverse proportionality with thickness. The highly nonlinear *i*/*V* curves observed with molecules present and their exponential thickness dependence are inconsistent with metal shorts or filaments. Finally, the decrease in conductance with temperature (Figure 7) for all junctions studied is opposite to the dependence expected for metals. While it is difficult to totally rule out the existence of metallic shorts in PPF/molecule/Cu crossed junctions, the observed structure, thickness, and temperature dependencies indicate strongly that shorts or pinholes cannot be a major factor controlling conductivity.

The observed junction capacitances of 2.1−3.3 μF at 100 kHz should be interpreted with caution, since they exhibited a frequency dependence. A wider frequency range will be necessary in order to determine if the frequency dependence is due to a property of the molecules or to a measurement error. However, it is still useful to consider if the observed values are within reasonable expectations for 1.5−4.5 nm thick junctions. Using a simple parallel plate capacitor model, the observed capacitances correspond to an upper limit of dielectric constants for the molecular layer in the range of 3.8−9.0, with the larger values observed for nitrobiphenyl. While these values are higher than most hydrocarbons, they occur for conjugated molecules oriented along their long axis, for which the molecular polarizability is a maximum.

Given the variation in organic film thickness resulting from diazonium modification, a cautionary note about film structure

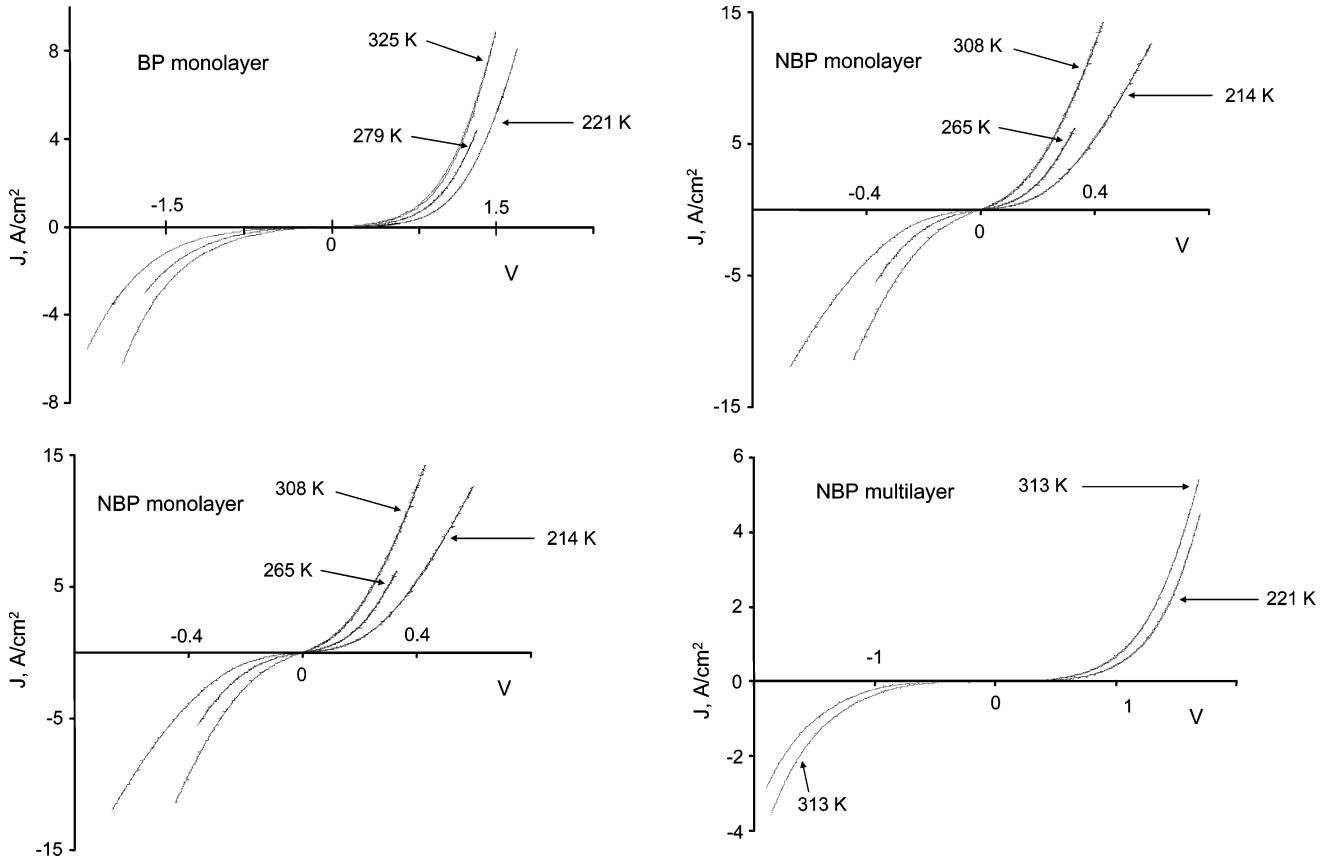

Figure 8. *i*/*V* curves obtained at 1000 V/s at the indicated temperatures for junctions made with biphenyl, fluorine, and nitrobiphenyl monolayers and for a 3.8 nm thick nitrobiphenyl multilayer.

is advisable. Although it is clear that diazonium reduction results in densely packed films with both monolayer and multilayer thicknesses, they are not as ordered as the more widely studied Au/thiol SAMs. The irreversible chemisorption of radicals generated by diazonium reduction prevents annealing over time, thus preventing formation of an ordered two-dimensional crystalline film. Furthermore, the PPF surface resembles a disordered glass with predominantly sp^2 hybridization.[71,73,74] However, it is still informative to compare the conductance of junctions with organic layers of different structure provided the disorder of the PPF or molecular layer is kept constant. For example, biphenyl and fluorene junctions are identical except for the bridging CH_2 group and ring coplanarity, and small differences in packing density could not account for the factor of ~10 difference in conductivity. Since PPF is a glass, it may not be possible to precisely determine the structure of the molecule/substrate interface, but it is both possible and valuable to investigate the effects of molecular structural changes on electronic behavior.

Before considering possible electron-transfer mechanisms through the molecular layer, several observations must be accounted for by any conduction model. First, conduction in monolayers is strongly dependent on structure, both the ring planarity noted above and the presence of a NO_2 group. The higher conductivity of NBP over BP is presumably due to a more covalent Cu−NO_2 interaction compared to Cu−phenyl, analogous to that observed when titanium is deposited on nitroazobenzene.[67,69] Second, although the conductance depends exponentially on the thickness of an NBP layer, the attenuation coefficient of 0.24 $Å^{-1}$ is small compared to that reported for phenylethynyl oligomers (0.3−0.6 $Å^{-1}$)[45−48] or alkanes (1.0 $Å^{-1}$). The observed attenuation factor is weakly dependent on voltage for NBP, decreasing to 0.20 $Å^{-1}$ at +0.5 V and 0.21 $Å^{-1}$ at −0.5 V. A similar attenuation factor was observed for electrochemical ET through a series of aromatic molecules on carbon electrodes for both $Ru(NH_3)_6^{3+/2+}$ (0.21 $Å^{-1}$) and chlorpromazine (0.20 $Å^{-1}$) redox systems in aqueous solution.[102,103] In addition, an STM study of conductance through single polyolefin molecules[104] of varying length reported an attenuation factor of 0.22 ± 0.04 $Å^{-1}$. Third, the conductance decreases with decreasing temperature but with a small apparent activation barrier. Preliminary estimates of activation barriers determined from plots of ln(conductance, ±50 mV) vs l/*T* over the 214−325 K temperature range are 0.064 eV for BP, 0.075 eV for FL, and 0.083 eV for NBP monolayers and 0.152 eV for NBP (3.8) multilayer. There is no obvious effect of structure on temperature dependence, with biphenyl, fluorine, and NBP monolayers having approximately equal barriers despite the differences in the Cu/molecule contact and in ring planarity. Fourth, plots of ln(*i*) vs *V* are nonlinear for all molecules and temperatures studied. Finally, if we assume that the $\sim 10^{10}$ molecules in a typical junction are acting as parallel resistors, the per-molecule resistance for the lowest resistance observed (258 Ω for NBP monolayer) would be 2.6×10^{12} Ω. This value is significantly higher than that reported for a single bipyridyl molecule (~10^7 Ω)[38,39] or a C_{12} alkane thiol (~10^{10} Ω).[18,55] Either the single molecule resistance does not scale linearly for parallel molecules due to lateral interactions (possibly coulombic), or for some reason only a subset of the 10^{10} is in contact electrically.

The *J*/*V* curve symmetry and small rectification ratios (1.1−2.2) are in contrast to those reported for rectifying molecular junctions.[27,65−67,105] The PPF/molecule/Cu junctions appear to be electronically symmetric, with weak or symmetric Schottky

barriers at the PPF/molecule and PPF/Cu (or Cu/Au) interfaces. The work functions of Cu (4.7 eV) and sp^2 hybridized carbon (4.8−5 eV) are similar,[106] with the slightly lower work function of Cu favoring electron injection from Cu rather than from PPF. However, the low rectification ratios indicate that the injection barriers at the "contacts" do not significantly affect the symmetry of the *J*/*V* curves.

We have previously reported on PPF/biphenyl/Hg junctions which have very similar construction to the current junctions, with the exception of top contact material and larger area (0.007 85 cm^2).[64] PPF/biphenyl/Hg junctions had an area-normalized low-voltage resistance of 108 $\Omega\cdot cm^2$ and a current density of 0.077 A/cm^2 at +0.5 V. Similarly, recently reported[68] PPF/biphenyl/Cu/Au junctions consisting of a 0.5 mm diameter spot rather than crossed-wire geometry had a low-voltage resistance of 0.62 $\Omega\cdot cm^2$ and a $J(+0.5V)$ of 0.83 A/cm^2. The area-normalized resistance of 1.61 $\Omega\cdot cm^2$ for the current crossed-wire junctions determined for the BP (1.5 nm) junctions listed in Table 2 is significantly lower than that observed for the analogous Hg junction and close to that of the Cu "spot". Similarly, the $J(+0.5V)$ for the crossed BP monolayer junctions (0.38 A/cm^2) is a factor of 5 higher than that of the Hg case and within a factor of 2.2 of the Cu spot. Given the possibility of uneven electrical contact of Hg across the BP monolayer, plus likely contamination of the Hg drop before making contact, it is not surprising that the Cu junctions exhibit higher conductivity at both low voltage and at +0.5 V. The reasons for the higher conductivity of the Cu spot compared to the crossed-junction geometry are not clear, but at least two measurement differences are present, and could account for the disparity. The crossed-junction geometry does not require a probe to make contact directly over the junction molecules, thus avoiding pressure or possible damage. The spot geometry does not readily permit correction for PPF resistance, as it can only be probed with a "two-wire" system.

As has been discussed in many reports, there are several electron transport mechanisms which may be invoked to explain the *i*/*V* characteristics of molecular junctions.[13,64,107−114] Although the current results do not yet permit identification of a specific mechanism operative in carbon/molecule/copper junctions, the results do provide some useful insights. As noted above, the strong dependence of conductivity on molecular structure clearly indicates that the major and possibly dominant factor controlling conductivity is molecular in origin, rather than some property of the carbon or metal layers. The weak temperature dependence implies that tunneling is important, particularly for junctions with molecular layers thinner than ∼2 nm. As an indication that coherent tunneling is at least possible for the monolayer junctions, the rectangular Simmons tunneling model[115,116] yields barrier heights of 1.99, 1.36, and 1.22 eV for BP(1.6), FL(1.7), and NBP(1.7) monolayer junctions, respectively. However, the weak thickness dependence observed for either BP or NBP is not compatible with coherent tunneling, nor is the observation of electron transport through >4 nm of the NBP multilayer. Incoherent (or "diffusive") tunneling[108,110,117−119] by a series of steps between potential wells does allow for transport across such large distances, with the potential wells possibly related to nitro groups in NBP or phenyl rings in BP.[120] It is possible that Schottky emission or the Poole−Frenkel effect are involved in transport, but the potential barriers would have to be quite small to account for the low observed activation barriers. Furthermore, these effects would not be expected to depend on molecular structure in the observed fashion and are not likely to be the dominant determinant of conductance. Electron transport mechanisms will continue to be a focus of ongoing research.

Conclusions

The carbon/molecule/Cu/Au "crossed-wire" junctions reported here are a robust and reproducible platform for the investigation of the effects of molecular structure on the electronic behavior of molecular junctions. The major effects of molecular structure and molecular layer thickness on junction conductance strongly support the contention that molecular structure is the primary determinant of the electronic properties of the junctions. The high yield and good reproducibility of the carbon-based molecular junctions are likely to be direct consequences of the strong C−C bond between the carbon substrate and the molecular layer, which reduces the incursion of vapor-deposited metals to a negligible level. The observed electron conduction through biphenyl, fluorene, and nitrobiphenyl monolayers and nitrobiphenyl multilayers is weakly temperature-dependent and can occur across layers as thick as 4.5 nm. A possible mechanism for electron transport in the carbon-based junctions is a combination of coherent or diffusive tunneling and a thermally activated process with a small activation barrier.

Acknowledgment. This work was supported by the National Science Foundation through Project 0211693 from the Analytical and Surface Chemistry Division.

References and Notes

(1) Zhou, C.; Deshpande, M. R.; Reed, M. A.; Jones, L.; Tour, J. M. *Appl. Phys. Lett.* **1997**, *71*, 611.
(2) Chang, S.-C.; Li, Z.; Lau, C. N.; Larade, B.; Williams, R. S. *Appl. Phys. Lett.* **2003**, *83*, 3198.
(3) Stewart, D. R.; Ohlberg, D. A. A.; Beck, P. A.; Chen, Y.; Williams, R. S.; Jeppesen, J. O.; Nielsen, K. A.; Stoddart, J. F. *Nano Lett.* **2004**, *4*, 133.
(4) Chen, Y.; Ohlberg, D. A. A.; Li, X.; Stewart, D. R.; Williams, R. S.; Jeppesen, J. O.; Nielsen, K. A.; Stoddart, J. F.; Olynick, D. L.; Anderson, E. *Appl. Phys. Lett.* **2003**, *82*, 1610.
(5) Chen, Y.; Jung, G.-Y.; Ohlberg, D. A. A.; Li, X.; Stewart, D. R.; Jeppesen, J. O.; Nielsen, K. A.; Stoddart, J. F.; Williams, R. S. *Nanotechnology* **2003**, *14*, 462.
(6) Jaiswal, A.; Amaresh, R. R.; Lakshmikantham, M. V.; Honciuc, A.; Cava, M. P.; Metzger, R. M. *Langmuir* **2003**, *19*, 9043.
(7) Slowinski, K.; Majda, M. *J. Electroanal. Chem.* **2000**, *491*, 139.
(8) Holmlin, R. E.; Haag, R.; Chabinyc, M. L.; Ismagilov, R. F.; Cohen, A. E.; Terfort, A.; Rampi, M. A.; Whitesides, G. M. *J. Am. Chem. Soc.* **2001**, *123*, 5075.
(9) Rampi, M. A.; Whitesides, G. M. *Chem. Phys.* **2002**, *281*, 373.
(10) Haag, R.; Rampi, M. A.; Holmlin, R. E.; Whitesides, G. M. *J. Am. Chem. Soc.* **1999**, *121*, 7895.
(11) Slowinski, K.; Fong, H. K. Y.; Majda, M. *J. Am. Chem. Soc.* **1999**, *121*, 7257.
(12) Tran, E.; Rampi, M. A.; Whitesides, G. M. *Angew. Chem., Int. Ed.* **2004**, *43*, 3835.
(13) Chen, J.; Calvet, L. C.; Reed, M. A.; Carr, D. W.; Grubisha, D. S.; Bennett, D. W. *Chem. Phys. Lett.* **1999**, *313*, 741.
(14) Chen, J.; Reed, M. A.; Rawlett, A. M.; Tour, J. M. *Science* **1999**, *286*, 1550.
(15) Mbindyo, J. K.; Mallouk, T. E.; Mattzela, J. B.; Kratochviloba, J.; Razavi, B.; Jackson, T. N.; Mayer, T. S. *J. Am. Chem. Soc.* **2002**, *124*, 4020.
(16) Cai, L. T.; Skulason, H.; Kushmerick, J. G.; Pollack, S. K.; Naciri, J.; Shashidhar, R.; Allara, D. L.; Mallouk, T. E.; Mayer, T. S. *J. Phys. Chem. B* **2004**, *108*, 2827.
(17) Kushmerick, J. G.; Allara, D. L.; Mallouk, T. E.; Mayer, T. S. *MRS Bull.* **2004**, 396.
(18) Cui, X. D.; Primak, A.; Zarate, X.; Tomfohr, J.; Sankey, O. F.; Moore, A. L.; Moore, T. A.; Gust, D.; Harris, G.; Lindsay, S. M. *Science* **2001**, *294*, 571.
(19) Wold, D. J.; Haag, R.; Rampi, M. A.; Frisbie, C. D. *J. Phys. Chem. B* **2002**, *106*, 2813.
(20) Cygan, M. T.; Dunbar, T. D.; Arnold, J. J.; Bumm, L. A.; Shedlock, N. F.; Burgin, T. P.; Jones, L.; Allara, D. L.; Tour, J. M.; Weiss, P. S. *J. Am. Chem. Soc.* **1998**, *120*, 2721.

(21) McCarty, G. S.; Weiss, P. S. *Chem. Rev.* **1999**, *99*, 1983.
(22) Donhauser, Z. J.; Mantooth, B. A.; Kelly, K. F.; Bumm, L. A.; Monnell, J. D.; Stapleton, J. J.; Price, D. W.; Rawlett, A. M.; Allara, D. L.; Tour, J. M.; Weiss, P. S. *Science* **2001**, *292*, 2303.
(23) Cui, X. D.; Primak, A.; Zarate, X.; Tomfohr, J.; Sankey, O. F.; Moore, A. L.; Moore, T. A.; Gust, D.; Nagahara, L. A.; Lindsay, S. M. *J. Phys. Chem. B* **2002**, *106*, 8604.
(24) Ramachandran, G. K.; Hopson, T. J.; Rawlett, A. M.; Nagahara, L. A.; Primak, A.; Lindsay, S. M. *Science* **2003**, *300*, 1413.
(25) Ramachandran, G. K.; Tomfohr, J. K.; Sankey, O. F.; Li, J.; Zarate, X.; Primak, A.; Terazano, Y.; Moore, T. A.; Moore, A. L.; Gust, D.; Nagahara, L. A.; Lindsay, S. M. *J. Phys. Chem. B* **2003**, *107*, 6162.
(26) Collier, C. P.; Mattersteig, G.; Wong, E. W.; Luo, Y.; Beverly, K.; Sampaio, J.; Raymo, F. M.; Stoddart, J. F.; Heath, J. R. *Science* **2000**, *289*, 1172.
(27) Metzger, R. M.; Xu, T.; Peterson, I. R. *J. Phys. Chem. B* **2001**, *105*, 7280.
(28) Metzger, R. M.; Chen, B.; Hopfner, U.; Lakshmikantham, M. V.; Vuillaume, D.; Kawai, T.; Wu, X.; Tachibana, H.; Hughes, T. V.; Sakurai, H.; Baldwin, J. W.; Hosch, C.; Cava, M. P.; Brehmer, L.; Ashwell, G. J. *J. Am. Chem. Soc.* **1997**, *119*, 10455.
(29) Chen, B.; Metzger, R. M. *J. Phys. Chem.* **1999**, *103*, 4447.
(30) Stewart, M. P.; Maya, F.; Kosynkin, D. V.; Dirk, S. M.; Stapleton, J. J.; McGuiness, C. L.; Allara, D. L.; Tour, J. M. *J. Am. Chem. Soc.* **2004**, *126*, 370.
(31) Wong, E. W.; Collier, C. P.; Behloradsky, M.; Raymo, F. M.; Stoddart, J. F.; Heath, J. R. *J. Am. Chem. Soc.* **2000**, *122*, 5831.
(32) Melosh, N. A.; Boukai, A.; Diana, F.; Gerardot, B.; Badolato, A.; Petroff, P. M.; Heath, J. R. *Science* **2003**, *300*, 112.
(33) Collier, C. P.; Jeppesen, J. O.; Luo, Y.; Perkins, J.; Wong, E. W.; Heath, J. R.; Stoddart, J. F. *J. Am. Chem. Soc.* **2001**, *123*, 12632.
(34) Rueckes, T.; Kim, K.; Joselevich, E.; Tseng, G. Y.; Cheung, C.; Lieber, C. M. *Science* **2000**, *289*, 94.
(35) Huang, Y.; Duan, X.; Wei, Q.; Lieber, C. M. *Science* **2001**, *291*, 630.
(36) Selzer, Y.; Cabassi, M. A.; Mayer, T. S.; Allara, D. L. *J. Am. Chem. Soc.* **2004**, *126*, 4052.
(37) Xiao, X.; Xu, B.; Tao, N. *Nano Lett.* **2004**, *4*, 267.
(38) Xiao, X.; Xu, B.; Tao, N. J. *Nano Lett.* **2004**, *4*, 267.
(39) Xu, B.; Tao, N. J. *Science* **2003**, *301*, 1221.
(40) Weiss, E. A.; Ratner, M. A.; Wasielewski, M. R. *J. Phys. Chem. A* **2003**, *107*, 3639.
(41) Segal, D.; Nitzan, A.; Davis, W. B.; Wasielewski, M. R.; Ratner, M. A. *J. Phys. Chem. B* **2000**, *104*, 3817.
(42) Lewis, F. D.; Liu, J.; Zuo, X.; Hayes, R. T.; Wasielewski, M. R. *J. Am. Chem. Soc.* **2003**, *125*, 4850.
(43) Davis, W. B.; Svec, W. A.; Ratner, M. A.; Wasielewski, M. R. *Nature* **1998**, *396*, 60.
(44) Sachs, S. B.; Dudek, S. P.; Hsung, R. P.; Sita, L. R.; Smalley, J. F.; Newton, M. D.; Feldberg, S. W.; Chidsey, C. E. D. *J. Am. Chem. Soc.* **1997**, *119*, 10563.
(45) Weber, K.; Hockett, L.; Creager, S. *J. Phys. Chem. B* **1997**, *101*, 8286.
(46) Creager, S.; Yu, C. J.; Bamdad, C.; O'Connor, S.; MacLean, T.; Lam, E.; Chong, Y.; Olsen, G. T.; Luo, J.; Gozin, M.; Kayyem, J. F. *J. Am. Chem. Soc.* **1999**, *121*, 1059.
(47) Sumner, J. J.; Weber, K. S.; Hockett, L. A.; Creager, S. E. *J. Phys. Chem. B* **2000**, *104*, 7449.
(48) Smalley, J. F.; Finkea, H. O.; Chidsey, C. E. D.; Linford, M. R.; Creager, S. E.; Ferraris, J. P.; Chalfant, K.; Zawodzinsk, T.; Feldberg, S. W.; Newton, M. D. *J. Am. Chem. Soc.* **2003**, *125*, 2004.
(49) Liu, B.; Bard, A. J.; Mirkin, M. V.; Creager, S. *J. Am. Chem. Soc.* **2004**, *126*, 1485.
(50) Fan, F.-R. F.; Yang, J.; Dirk, S. M.; Price, D. W.; Kosynkin, D.; Tour, J. M.; Bard, A. J. *J. Am. Chem. Soc.* **2001**, *123*, 2454.
(51) Fan, F.-R. F.; Yang, J.; Cai, L.; Price, D. W.; Dirk, S. M.; Kosynkin, D.; Yao, Y.; Rawlett, A. M.; Tour, J. M.; Bard, A. J. *J. Am. Chem. Soc.* **2002**, *124*, 5550.
(52) Fan, F.-R. F.; Lai, R. Y.; Cornil, J.; Karzazi, Y.; Brédas, J.-L.; Cai, L.; Cheng, L.; Yao, Y.; David W. Price, J.; Dirk, S. M.; Tour, J. M.; Bard, A. J. *J. Am. Chem. Soc.* **2004**, *126*, 2568.
(53) Fan, F.-R. F.; Yao, Y.; Cai, L.; Cheng, L.; Tour, J. M.; Bard, A. J. *J. Am. Chem. Soc.* **2004**, *126*, 4035.
(54) Engelkes, V. B.-. Beebe, J. M.; Frisbie, C. D. *J. Am. Chem. Soc.* **2004**, ASAP.
(55) Rawlett, A. M.; Hopson, T. J.; Nagahara, L. A.; Tsui, R. K.; Ramachandran, G. K.; Lindsay, S. M. *Appl. Phys. Lett.* **2002**, *81*, 3043.
(56) Lee, J.-O.; Lientschnig, G.; Wiertz, F.; Struijk, M.; Janssen, R. A.; Egberink, R.; Reinhoudt, D.; Hadley, P.; Dekker, C. *Nano Lett.* **2003**, *3*, 113.
(57) Haynie, B. C.; Walker, A. V.; Tighe, T. B.; Allara, D. L.; Winograd, N. *Appl. Surf. Sci.* **2003**, *203*−*204*, 433.
(58) Fisher, G. L.; Walker, A. V.; Hooper, A. E.; Tighe, T. B.; Bahnck, K. B.; Skriba, H. T.; Reinard, M. D.; Haynie, B. C.; Opila, R. L.; Winograd, N.; Allara, D. L. *J. Am. Chem. Soc.* **2002**, *124*, 5528.
(59) Fisher, G. L.; Hooper, A. E.; Opila, R. L.; Jung, D. R.; Allara, D. L.; Winograd, N. *J. Phys. Chem. B* **2000**, *104*, 3267.
(60) Fisher, G. L.; Hooper, A.; Opila, R. L.; Jung, D. R.; Allara, D. L.; Winograd, N. *J. Electron Spectrosc. Relat. Phenom.* **1999**, *98*−*99*, 139.
(61) Hooper, A.; Fisher, G. L.; Konstadinidis, K.; Jung, D.; Nguyen, H.; Opila, R.; Collins, R. W.; Winograd, N.; Allara, D. L. *J. Am. Chem. Soc.* **1999**, *121*, 8052.
(62) Ranganathan, S.; Steidel, I.; Anariba, F.; McCreery, R. L. *Nano Lett.* **2001**, *1*, 491.
(63) Solak, A. O.; Ranganathan, S.; Itoh, T.; McCreery, R. L. *Electrochem. Solid State Lett.* **2002**, *5*, E43.
(64) Anariba, F.; McCreery, R. L. *J. Phys. Chem. B* **2002**, *106*, 10355.
(65) McCreery, R. L.; Dieringer, J.; Solak, A. O.; Snyder, B.; Nowak, A.; McGovern, W. R.; DuVall, S. *J. Am. Chem. Soc.* **2003**, *125*, 10748.
(66) McCreery, R.; Dieringer, J.; Solak, A. O.; Snyder, B.; Nowak, A. M.; McGovern, W. R.; DuVall, S. *J. Am. Chem. Soc.* **2004**, *126*, 6200.
(67) Nowak, A.; McCreery, R. *J. Am. Chem. Soc.* **2004**, *126*, 16621.
(68) McGovern, W. R.; Anariba, F.; McCreery, R. L. *J. Electrochem. Soc.*, in press.
(69) Nowak, A. M.; McCreery, R. L. *Anal. Chem.* **2004**, *76*, 1089.
(70) McCreery, R. Special Issue: Molecular Electronics. *Electrochem. Soc. Interface* **2004**, *13*, 46.
(71) Kostecki, R.; Schnyder, B.; Alliata, D.; Song, X.; Kinoshita, K.; Kotz, R. *Thin Solid Films* **2001**, *396*, 36.
(72) Kostecki, R.; Song, X.; Kinoshita, K. *Electrochem. Solid State Lett.* **1999**, *2*, 465.
(73) Ranganathan, S.; McCreery, R. L. *Anal. Chem.* **2001**, *73*, 893.
(74) Ranganathan, S. Preparation, Modification and Characterization of a Novel Carbon Electrode Material for Applications in Electrochemistry and Molecular Electronics. Ph.D. Thesis, The Ohio State University, Columbus, OH, 2001.
(75) Adenier, A.; Bernard, M.-C.; Chehimi, M. M.; Cabet-Deliry, E.; Desbat, B.; Fagebaume, O.; Pinson, J.; Podvorica, F. *J. Am. Chem. Soc.* **2001**, *123*, 4541.
(76) Allongue, P.; Delamar, M.; Desbat, B.; Fagebaume, O.; Hitmi, R.; Pinson, J.; Saveant, J. M. *J. Am. Chem. Soc.* **1997**, *119*, 201.
(77) Andrieux, C. P.; Pinson, J. *J. Am. Chem. Soc.* **2003**, *125*, 14801.
(78) Bernard, M.-C.; Chausse, A.; Cabet-Deliry, E.; Chehimi, M. M.; Pinson, J.; Podvorica, F.; Vautrin-Ul, C. *Chem. Mater.* **2003**, *15*, 3450.
(79) Boukerma, K.; Chehimi, M. M.; Pinson, J.; Blomfield, C. *Langmuir* **2003**, *19*, 6333.
(80) Chausse, A.; Chehimi, M. M.; Karsi, N.; Pinson, J.; Podvorica, F.; Vautrin-Ul, C. *Chem. Mater.* **2002**, *14*, 392.
(81) Coulon, E.; Pinson, J.; Bourzat, J.-D.; Commercon, A.; Pulicani, J.-P. *J. Org. Chem.* **2002**, *67*, 8513.
(82) Coulon, E.; Pinson, J.; Bourzat, J.-D.; Commercon, A.; Pulicani, J.-P.; *Langmuir* **2002**, *17*, 7102.
(83) de Villeneuve, C. H.; Pinson, J.; Bernard, M. C.; Allongue, P. *J. Phys. Chem. B* **1997**, *101*, 2415.
(84) Delamar, M.; Desarmot, G.; Fagebaume, O.; Hitmi, R.; Pinson, J.; Saveant, J. *Carbon* **1997**, *35*, 801.
(85) Delamar, M.; Hitmi, R.; Pinson, J.; Saveant, J. M. *J. Am. Chem. Soc.* **1992**, *114*, 5883.
(86) Toupin, M.; Brousse, T.; Belanger, D. *Chem. Mater.* **2004**, *16*, 3184.
(87) Ortiz, B.; Saby, C.; Champagne, G. Y.; Belanger, D. *J. Electroanal. Chem.* **1998**, *455*, 75.
(88) Saby, C.; Ortiz, B.; Champagne, G. Y.; Belanger, D. *Langmuir* **1997**, *13*, 6805.
(89) Brooksby, P. A.; Downard, A. J. *Langmuir* **2004**, *20*, 5038.
(90) Downard, A. J. *Electroanalysis* **2000**, *12*, 1085.
(91) Downard, A. J. *Langmuir* **2000**, *16*, 9680.
(92) Liu, Y.-C.; McCreery, R. L. *J. Am. Chem. Soc.* **1995**, *117*, 11254.
(93) Liu, Y.-C.; McCreery, R. L. *Anal. Chem.* **1997**, *69*, 2091.
(94) Anariba, F.; DuVall, S. H.; McCreery, R. L. *Anal. Chem.* **2003**, *75*, 3837.
(95) Kushmerick, J. G.; Holt, D. B.; Yang, J. C.; Naciri, J.; Moore, M. H.; Shashidhar, R. *Phys. Rev. Lett.* **2002**, *89*, 086802.
(96) McAlpine, M. C.; Friedman, R. S.; Jin, S.; Lin, K.-h.; Wang, W. U.; Lieber, C. M. *Nano Lett.* **2003**, *3*, 1531.
(97) Ranganathan, S.; McCreery, R. L.; Majji, S. M.; Madou, M. *J. Electrochem. Soc.* **2000**, *147*, 277.
(98) Kariuki, J. K.; McDermott, M. T. *Langmuir* **1999**, *15*, 6534.
(99) Kariuki, J. K.; McDermott, M. T. *Langmuir* **2001**, *17*, 5947.
(100) Combellas, C.; Kanoufi, F.; Pinson, J.; Podvorica, F. *Langmuir* **2005**, *21*, 280.
(101) Lindsay, S. M. *Interface* **2004**, *13*.
(102) Yang, H.-H. The Effects of Modified Glassy Carbon Surfaces on Electron-Transfer Kinetics of Organic Redox Systems. The Ohio State University, Columbus, OH, 2000.
(103) Yang, H.-H.; McCreery, R. L. *Anal. Chem.* **1999**, *71*, 4081.

(104) He, J.; Chen, F.; Li, J.; Sankey, O.; Terazono, Y.; Herroro, C.; Gust, D.; Moore, T.; Moore, A. L.; Lindsay, S. M. *J. Am. Chem. Soc.* **2005**, *127*, 1384.

(105) Metzger, R. M.; Baldwin, J. W.; Shumate, W. J.; Peterson, I. R.; Mani, P.; Mankey, G. J.; Morris, T.; Szulczewski, G.; Bosi, S.; Prato, M.; Commito, A.; Rubin, Y. *J. Phys. Chem. B* **2003**, *107*, 1021.

(106) Weast, R. C. *CRC Handbook of Chemistry and Physics*, 66th ed.; CRC Press: Boca Raton, FL, 1985.

(107) McCreery, R. *Chem. Mater.* **2004**, *16*, 4477.

(108) Nitzan, A.; Ratner, M. A. *Science* **2003**, *300*, 1384.

(109) Heath, J. R.; Ratner, M. A. *Phys. Today* **2003**, *56*, 43.

(110) Mujica, V.; Ratner, M. A. *Chem. Phys.* **2001**, *264*, 365.

(111) Yaliraki, S. N.; Roitberg, A. E.; Gonzalez, C.; Mujica, V.; Ratner, M. A. *J. Phys. Chem.* **1999**, *111*, 6997.

(112) Jortner, J.; Ratner, M. *Molecular Electronics*; Blackwell Science Ltd.: Berlin, 1997.

(113) *Molecular Nanoelectronics*; Reed, M. A., Lee, T., Eds.; American Scientific Publishers: Stevenson Ranch, CA, 2003.

(114) Reed, M. A.; Zhou, C.; Muller, C. J.; Burgin, T. P.; Tour, J. M. *Science* **1997**, *278*, 252.

(115) York, R. L.; Slowinski, K. *J. Electroanal. Chem* **2003**, *550*−*551*, 327.

(116) Simmons, J. G. *DC Conduction in Thin Films*; Mills and Boon Ltd.: London, 1971.

(117) Mujica, V.; Kemp, M.; Roitberg, A.; Ratner, M. *J. Chem. Phys.* **1996**, *104*, 7296.

(118) Mujica, V.; Roitberg, A. E.; Ratner, M. A. *J. Phys. Chem.* **2000**, *112*, 6834.

(119) Nitzan, A. *Annu. Rev. Phys. Chem.* **2001**, *52*, 681.

(120) Berlin, Y. A.; Hutchison, G. R.; Rempala, P.; Ratner, M. A.; Michl, J. *J. Phys. Chem. A* **2003**, *107*, 3970.